genesis 26:265–270 (2000)

LETTER

Cerberus-like Is a Secreted BMP and Nodal Antagonist Not Essential for Mouse Development

José António Belo,[1,2]* D. Bachiller,[1] E. Agius,[2] C. Kemp,[1] A.C. Borges,[2] S. Marques,[2] S. Piccolo,[1] and Eddy M. De Robertis[1]

[1]Howard Hughes Medical Institute, Department of Biological Chemistry, University of California, Los Angeles, California
[2]Instituto Gulbenkian de Ciência, Oeiras, Portugal

Received 8 February 2000; Accepted 10 February 2000

Summary: Mouse *cerberus-like (cer-l)* is a member of the *Cerberus/Dan* family of secreted factors. As other members of this family of proteins, Cer-l functions in the extracellular space, inhibiting signaling molecules. Here we show that the neural-inducing and mesoderm-inhibiting activities of Cer-l result from specific binding to BMP and Nodal molecules, respectively. These properties resemble the ones from the related factor *Xenopus* Cerberus. However, *Xenopus* Cerberus in addition to BMP4 and Nodal also binds to and inhibits Wnt proteins. We show that Cer-l does not directly inhibit Wnt signals. A null allele of the mouse *Cer-l* gene was generated by targeted inactivation in ES cells. Homozygous embryos show no anterior patterning defects, are born alive, and are fertile. Since mouse Cer-l and *Xenopus* Cerberus differ in biochemical activities, we propose the existence of additional members of this family of inhibitors, which may compensate for the loss of *cer-l*. genesis 26: 265–270, 2000. © 2000 Wiley-Liss, Inc.

Key words: *cerberus-like*; Cerberus; nodal; AVE; head induction

Mouse *cerberus-like* mRNA has been shown to be a potent neural inducer in *Xenopus* assays (Belo *et al.,* 1997; Biben *et al.,* 1998), inducing the same set of anterior neural markers as the related head-inducing molecule *Xenopus cerberus* (Bouwmeester *et al.,* 1996; Piccolo *et al.,* 1999). It has been suggested that this property could result from the inhibition of BMP signaling (Biben *et al.,* 1998; Hsu *et al.,* 1998; Pearse *et al.,* 1999), as it is the case for the *Xenopus* neural-inducing molecules Chordin and Noggin (Piccolo *et al.,* 1996; Zimmerman *et al.,* 1996).

To determine the molecular mechanism of the *cer-l* neural-inducing activity, we prepared soluble Cer-l protein by transfection of human 293T cells. The protein was secreted into the culture medium as a product of 40–45 kDa that forms dimers under nonreducing conditions (data not shown) and was able to block BMP4 protein signaling in a dissociated animal cap assay (Wilson and Hemmati-Brivanlou, 1995; Piccolo *et al.,* 1996). In this assay, the neuralization caused by the dispersal of the inner layer of the animal cap is prevented by the addition of BMP4, which acts as an epidermal (*keratin*) inducer. Animal caps were cut at stage 9, the outer layer manually removed, and the inner cells were dissociated in a calcium magnesium-free medium for 4 h in presence or absence of protein (Fig. 1A). After 4 h, the inner cells were reaggregated by addition of calcium and magnesium to the medium and cultured until stage 20 to be processed for RT-PCR (Fig. 1B). Dissociated cells express *NCAM* but not *cytokeratin* (Fig. 1B, lane 2). In the presence of 2 nM of BMP4 protein, the dissociated cells retain their epidermal state, expressing *cytokeratin* but not *NCAM* (Fig. 1B, lane 3). A mixture of Mcer-l and BMP4 proteins (10 nM and 2 nM, respectively) prevents BMP4 to act as an anti-neural reagent and restores the *NCAM* expression in the animal cap cells (Fig. 1B, lane 4).

To test the level at which this inhibition takes place, we performed an epistatic experiment in which *cer-l* mRNA was co-injected into Xenopus embryos with either BMP4 or a constitutively active form of BMP4 receptor (*CABMPR)* mRNA. Injections into all animal blastomeres were done at 8-cell stage, animal caps were cut at blastula, harvested at stage 27, and analyzed by RT-PCR (Fig. 1C). Microinjection of *cer-l* mRNA (800 pg) induced the expression of *NCAM* in animal caps (Fig. 1C, lane 3). Co-injection with *BMP4* mRNA did not prevent *NCAM* expression, whereas co-injection with *CA-BMPR* mRNA abolished *NCAM* expression (Fig. 1C, lanes 4, 5). We conclude from these results that Cer-l acts extracel-

* Correspondence to: José António Belo, Instituto Gulbenkian de Ciência, Rua da Quinta Grande, 6, Apartado 14, 2780-156 Oeiras, Portugal.
E-mail: jbelo@igc.gulbenkian.pt
Current address: E. Agius, Cent. Biol. Dével., Université Paul Sabatier, 31062 Toulouse, France.
Current address: S. Piccolo, Dipart. di Biotecnol. Mediche, Universitè di Padova, 35100 Padova, Italy.
Contract grant sponsor: FLAD research fellowship, Contract grant sponsor: HHMI, Contract grant sponsor: Sprague Endowment, Contract grant sponsor: Fundação Calouste Gulbenkian/Instituto Gulbenkian de Ciência.

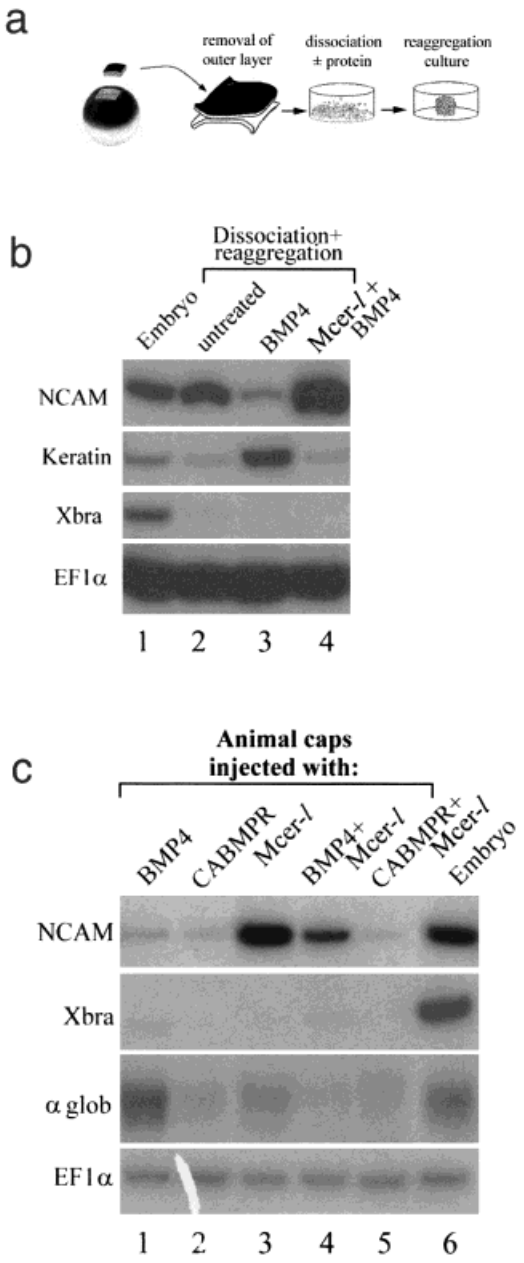

FIG 1. Mouse Cerberus-like (Cer-l) blocks BMP4 signaling extracellularly. **(a, b)** Mouse Cer-l protein blocks BMP4 protein signaling in animal cap cells dissociated for 4 h:. A, experimental design; B, RT-PCR analysis of the dissociation experiment. Lane 1, control embryos at stage 18. Lane 2, dissociated and reaggregated cells; NCAM is induced. Lane 3, addition of 2 nM of BMP4 protein; NCAM is repressed. Lane 4, addition of 10 nM mouse Cer-l and 2 nM BMP4 protein; Cer-l protein blocks the activity of the BMP4 protein. The pan-mesodermal marker *Xbra* is not affected. *EF1a* is used as a loading control. **(c)** *cer-l* blocks *BMP* signaling upstream of the *BMP* receptor. Molecular markers were analyzed in animal explants at stage 27 following mRNA microinjection. Lane 1, *BMP4* (300 pg). Lane 2, *CA-BMPR* (300 pg). Lane 3, mouse *cer-l* (800 pg). Lane 4, *BMP4* co-injected with 800 pg of *cer-l* mRNA. Lane 5, *CA-BMPR* co-injected with *cer-l;* note that neural induction by *cer-l* is abolished. Lane 6, control embryo. In this experiment, the amount of *BMP4* mRNA injected was substantial, as indicated by the induction of the ventral mesodermal marker *α-globin* in lane 1, which was even higher than the induction caused by CA-BMPR alone in lane 2.

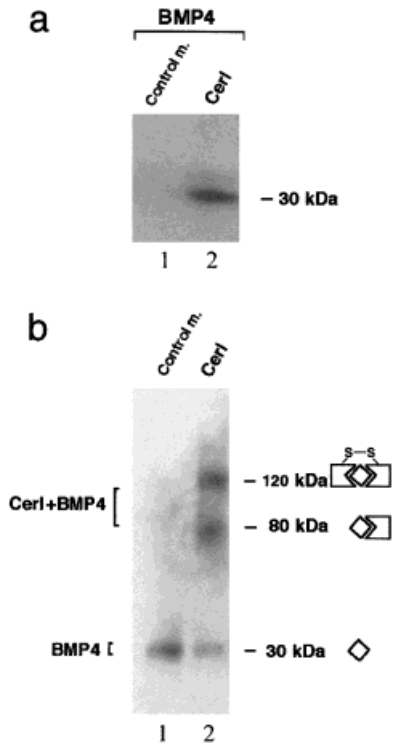

FIG. 2. Mouse Cerberus-like binds BMP-4. **(a)** Co-immunoprecipitation of Cer-l and BMP4 with anti-HA antibody followed by detection with anti-BMP4 monoclonal antibody. Lane 1, 5 nM of BMP4 protein and control medium. Lane 2, 5 nM BMP4 protein with 20 nM Cer-l-HA protein. **(b)** Cross-linking of Cer-l-HA/BMP-4 complexes using DSP and detection with anti-BMP4 monoclonal antibody. Lane 1, BMP4 protein with control medium. Lane 2, BMP4 dimers form two complexes with Cer-l monomers and dimers that run as 80- and 120-kDa complexes, respectively. Protein concentrations were the same as in A.

lularly and upstream of the BMP4 receptor, probably by binding to BMP4.

To test this directly, we constructed an expression vector in which Cer-l was tagged at the carboxy-terminus with the hemagglutinin (HA) epitope. Soluble Cer-l-HA protein was obtained by transfecting human 293T cells and used in co-immunoprecipitation experiments. A mixture of Cer-l-HA and BMP4 proteins (20 nM and 5 nM, respectively) was incubated at room temperature and immunoprecipitated with anti-HA antibody. BMP4 was indeed bound by Cer-l, as detected on a Western blot by a monoclonal anti-BMP4 antibody (Fig. 2A). To prove that the binding is direct, dithiobis (succinimidyl) propionate (DSP) was used to chemically cross-link Cer-l-HA/BMP-4 complexes. After separation in nonreducing SDS polyacrylamide gels, the products of the reaction were visualized on Western blots with anti-BMP4 monoclonal antibody. As shown in Figure 2B, Cer-l bound to BMP4 protein both as a monomer and as a dimer. This strongly suggests that the neuralizing activity of Cer-l results from direct binding to BMP4, thus preventing activation of the BMP4 receptor.

Injection of *Mcer-l* mRNA in *Xenopus* embryos also results in enlarged dorso-anterior structures and shortened body axes (Belo *et al.,* 1997), indicating some degree of mesoderm inhibition. The related cerberus (Xcer) protein has been shown to be a potent mesoderm inhibitor by blocking the Nodal and Wnt pathways (Piccolo *et al.,* 1999). To determine whether Cer-l blocks the Nodal pathway, we assayed the effects of Xnr-1 protein (*Xenopus* Nodal related-1) in animal cap cells. When these cells were incubated in the presence of 2 nM Xnr-1, the mesodermal markers *Xbra* and *Xwnt-8* were induced (Fig. 3A, lane 3). However, in cells incubated with 2 nM Xnr-1 and 5 nM mouse Cer-l or *Xenopus* Cerberus proteins, the induction of these mesodermal markers was abolished (Fig. 3A, lanes 4, 5).

To test whether the inhibition of Xnr-1 took place upstream or downstream of the *nodal* receptor, we performed epistatic experiments with a constitutively active form of the activin receptor (*CA-ALK4*; Chang *et al.,* 1997). Microinjection of animal caps with mouse *Nodal* or *Xnr-1* mRNA (Fig. 3B, lanes 4, 6, respectively) induced the expression of *Xbra* and *Sox17β,* a pan-endodermal marker. Co-injection of mouse *cer-l* mRNA completely blocked mouse *Nodal* activity and inhibited *Xnr-1* as well (Fig. 3B, lanes 5, 7). Injection of *CA-ALK4* also leads to the induction of *Xbra* and *Sox17β.* This activity could not be prevented by co-injection with mouse *cer-l* mRNA (Fig. 3B, lanes 8, 9). This experiment suggests that *cer-l* inhibits *nodal* signaling extracellularly, upstream of the receptor.

To investigate whether *cer-l* is also able to block the Wnt pathway, we first performed microinjections into *Xenopus* embryos. Although we observed that mouse *cer-l* mRNA antagonized secondary axis formation by *Xwnt-8* (data not shown), we reasoned that this could be due to the mesoderm-inhibiting (anti-Nodal) activity of Cer-l, rather than to a direct effect on the Wnt pathway itself. To test this, we performed a set of epistatic experiments in animal caps using the direct downstream targets of Wnt signaling *Siamois* and *Xnr-3* as reporters of Wnt pathway activity (Brannon *et al.,* 1997; McKendry *et al.,* 1997). We confirmed that *Xenopus cerberus* mRNA is able to inhibit *Xwnt-8* but not *β-catenin* signaling (Piccolo *et al.,* 1999; Fig. 4E, lanes 7, 10). However, we found that *cer-l* mRNA (even at high doses of 600 pg) was unable to block *Xwnt-8* signals (Fig. 4E, lane 6). We conclude from these experiments that mouse *cer-l* does not inhibit *Xwnt-8* signaling directly. Therefore, mouse *cerberus-like* is an antagonist of Nodal and BMP signals but not of Wnts.

During early development, *cer-l* is expressed in the Anterior Visceral Endoderm (AVE) of the pre-streak mouse embryo (Belo *et al.,* 1997; Biben *et al.,* 1998; Shawlot *et al.,* 1998). The AVE has been proposed to be important for anterior neural induction (Thomas and Beddington, 1996; Bouwmeester and Leyns, 1997). This, together with the neuralizing activity of *cer-l* in *Xenopus* overexpression assays and the ability of Cer-l protein to bind BMP4, suggested a role for *cer-l* in head formation.

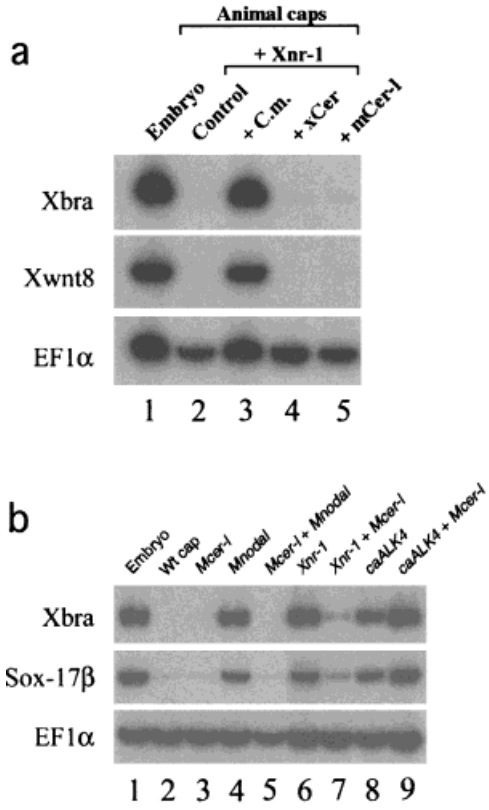

FIG. 3. Inhibition of *nodal* signals by mouse *cer-l.* **(a)** Mouse Cer-l protein blocks signaling by Xnr-1 protein in animal cap cells. Animal caps were cut at stage 8, incubated in the absence (lane 2) or presence (lanes 3–5) of 2 nM Xnr-1 protein until early gastrula, and processed for RT-PCR. Lane 1, control embryo. Lane 2, animal caps incubated with control conditioned medium. Lane 3, animal caps incubated with 2 nM Xnr-1. Lane 4, animal caps incubated with 2 nM Xnr-1 and 5 nM *Xenopus* Cerberus protein. Lane 5, animal caps incubated with Xnr-1 and 5 nM mouse Cer-l protein. Note the lack of induction of the mesodermal marker *Xbra*. *EF1α was used as a loading control.* **(b)** *cer-l* mRNA is an inhibitor of mouse Nodal signaling in the *Xenopus* animal cap assay. Lane 1, control embryo. Lane 2, control animal caps. Lane 3, animal cap injected with *cer-l* (600 pg). Lane 4, injection of mouse *Nodal* mRNA (50 pg) in animal caps. Lane 5, co-injection of mouse *cer-l* and *Nodal* mRNAs. Lane 6, injection of *Xnr-1* (50 pg). Lane 7, co-injection of *cer-l* with *Xnr-1.* Lane 8, injection *of CA-ALK4* (400 pg). Lane 9, co-injection of *cer-l* with *CA-ALK4*. Cer-l inhibits Nodal activity but does not prevent signaling by *CA-ALK4*, suggesting that *cer-l* acts upstream of the receptor.

To determine the requirement of *cer-l* during mouse development, we generated a null allele of the gene by deleting most of the first and the entire second exon (Fig. 5A). Cell lines that had undergone homologous recombination were identified by Southern blot and one of them injected into C57BL/6 blastocysts. The chimeric males obtained were subsequently mated with wild-type 129/Sv or C57BL/6 females.

cer-l$^{+/-}$ animals in the 129/Sv pure inbred background were intercrossed and the offspring genotyped by Southern and PCR analysis (Fig. 5B, C). Homozygous mutant pups were recovered at a mendelian ratio (28 of

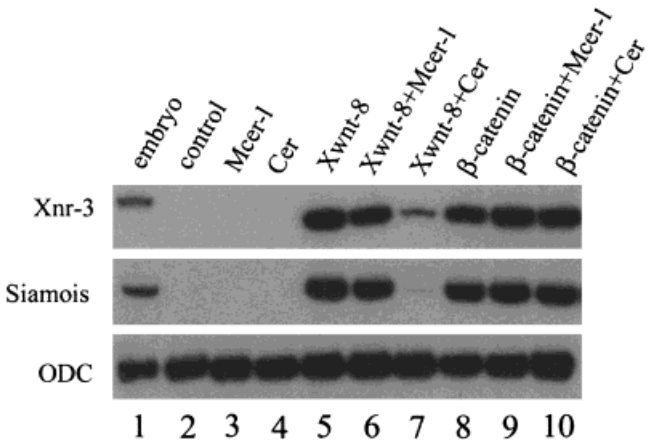

FIG. 4. Inhibition of *Wnt* signaling by *Xenopus cerberus* but not by mouse *cerberus-like*. Lane 1, control embryo. Lane 2, control stage 10 animal caps. Lane 3, animal cap microinjected with *cer-l* mRNA (600 pg). Lane 4, microinjection of *Xenopus cerberus* (600 pg). Lane 5, injection of *Xwnt-8* (80 pg). Lane 6, co-injection of *Xwnt-8* with *cer-l;* note that mouse *cer-l* does not inhibit expression of Siamois and Xnr-1. Lane 7, co-injection of *Xwnt-8* with *Xenopus cerberus;* Wnt signaling is inhibited. Lane 8, microinjection of the downstream Wnt pathway component *β-catenin* (600 pg). Lane 9, co-injection of *β-catenin* with *cer-l.* Lane 10, co-injection of *β-catenin* with *Xenopus cerberus*. *ODC* serves as loading control.

107). Careful morphological analysis revealed no major abnormality in them (Fig. 5D, E). Furthermore, *cer-l*$^{-/-}$ adult animals appeared normal and were fertile. To test whether there was some effect due to genetic background, *cer-l*$^{+/-}$ males of 129/Sv x C57BL/6 hybrid background were backcrossed for four generations with C57BL/6 females. Intercrosses of heterozygous F4 animals led to the same results obtained with the pure 129/Sv inbred background. These data confirm a recent report indicating that a large deletion encompassing the *cer-l* locus had minor influence on mouse development (Simpson *et al.,* 1999) and is further supported by two independent reports in this issue.

In conclusion, mouse *cer-l* shares some activities with the related gene *Xenopus cerberus.* Nevertheless, differences do exist: *Xenopus cerberus* is a triple inhibitor of Nodal, BMPs, and Wnt signaling, whereas we show here that *cer-l* cannot block *Xwnt-8* activity. In fact, almost no similarities are found between these two proteins in the amino-terminal region required for Wnt binding (Belo *et al.,* 1997; Piccolo *et al.,* 1999). In view of the functional differences reported here, it is conceivable that a murine homologue of *Xenopus cerberus* and/or other members of the *cerberus/Dan* gene family (Hsu *et al.,* 1998; Pearse *et al.,* 1999; Rodriguez-Esteban *et al.,* 1999; Yokouchi *et al.,* 1999; Zhu *et al.,* 1999), may exist in mouse that compensate for the lack of *cer-l* activity in *cer-l*$^{-/-}$ animals. There is a precedent for this type of compensation, as exemplified by the case of the BMP antagonists *chordin* and *noggin*, for which double mutants are required to reveal strong anterior neural phenotypes (Bachiller *et al.,* 2000).

METHODS

DNA Expression Constructs

An HA-tagged version of the full-length *cer-l* cDNA (pCS2-*Mcerl*-HA) was constructed by PCR. The sequence YPYDVPDYA-Stop was added after the last amino acid of *cer-l* and the entire sequence inserted into pCS2. To generate an active form of mouse Nodal, we used pCS2-*proAct,* an expression vector containing the pre-pro region and proteolytic cleavage site of activin-βB (Kessler and Melton, 1995; Piccolo *et al.,* 1999). A PCR fragment encoding the mature region of mouse Nodal (starting at residue H242) was generated by PCR amplification using primers flanked by *Xho*I and *Xba*I sites and subcloned into pCS2-*proAct*, resulting in the pCS2-*ActβB-Mnodal* plasmid. *cer-l-HA* and *ActβB-Mnodal* sense mRNA were synthesized using SP6 polymerase after linearization with *Not*I (Bouwmeester *et al.,* 1996). All other mRNAs used in microinjection experiments were generated and microinjected as described by Piccolo *et al.* (1999).

Cell Culture and Protein Binding

Soluble Cer-l and Cer-l-HA proteins were obtained by transfection of embryonic human kidney cells (293T) as described (Belo *et al.,* 1997). Production of soluble Cer and Xnr-1 proteins by secretion of manually defolliculated *Xenopus* oocytes, protein incubation, and binding experiments were performed as described (Piccolo *et al.,* 1999).

Generation of Chimeric Mice

cer-l cDNA was used to screen a 129/Sv mouse genomic DNA λ phage library (Stratagene) and resulted in the isolation of two 6.0 kb *Eco*RI fragments. The targeting construct was generated in the pPNT plasmid (Tybulewicz *et al.,* 1991) by replacing a 3.5-kb *Bgl* II/*Kpn* I fragment containing most of the exon I and the entire exon II by an IRES-lacZ-Neo cassette. This was flanked by a homologous 2.5-kb 5′ region and a homologous 3.0-kb 3′ region. An HSV-TK cassette was inserted at the end of the 3′ arm for negative selection, generating the targeting vector pPNT-McerlKO. The IRES-lacZ-Neo cassette introduced novel endonuclease restriction sites. Regrettably, the IRES sequence used in this construction had a deletion of several nucleotides, and the targeted strain did not express *lacZ*.

pPNT.McerlKO was linearized at a unique *Not*I site and electroporated into RW-4 ES cells (Genome Systems). G418-resistant colonies were isolated and analyzed for correct homologous recombination. ES cell manipulation, recombination, and generation of chimeric mice were done as described (Robertson *et al.,* 1987). Alcian blue-alizarin red skeletal staining was performed as previously described (Belo *et al.,* 1998) and images were acquired using a Leica DC 200 digital camera.

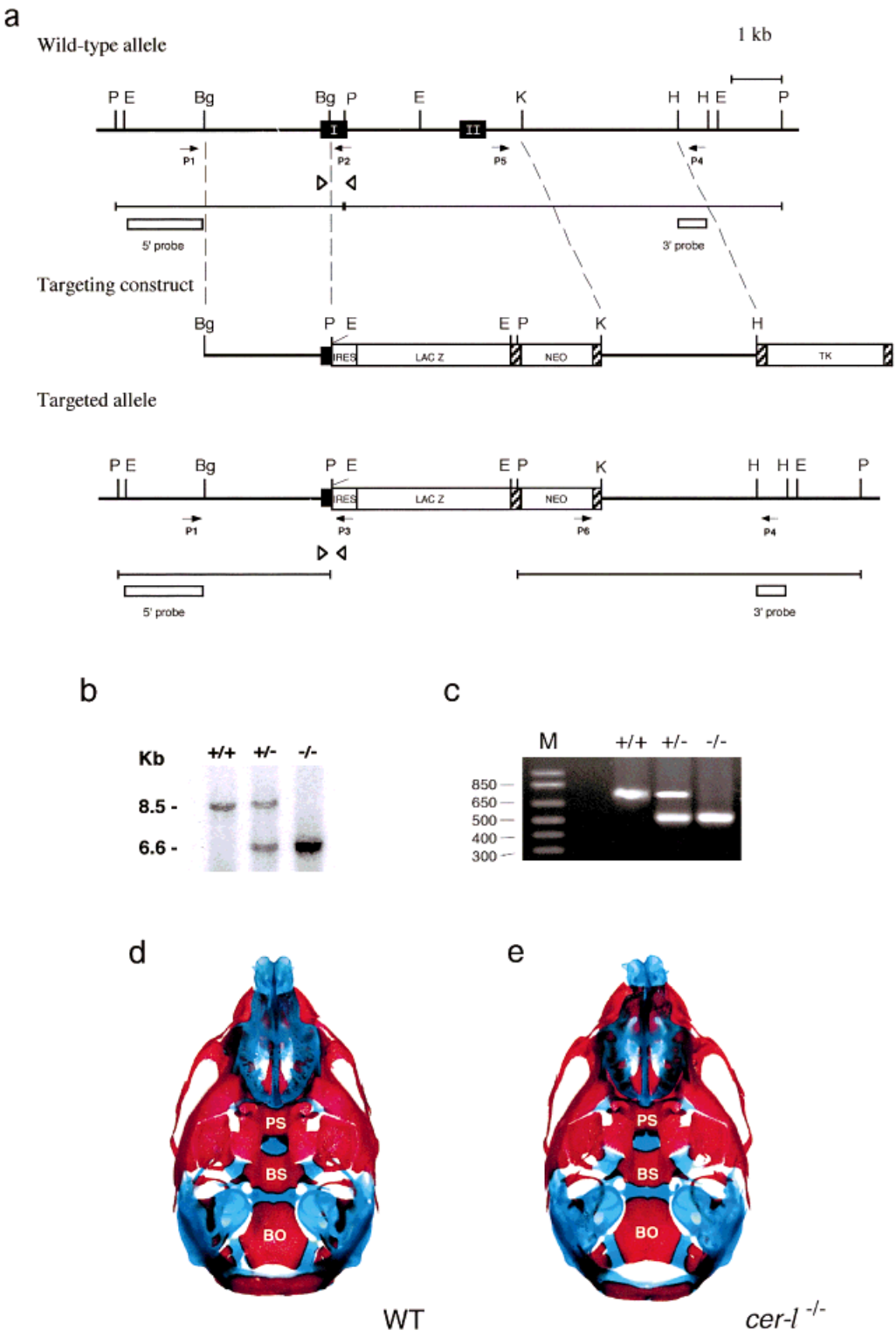

FIG. 5. A targeted null mutation of the mouse *cerberus-like* gene. **(a)** Schematic representation of the targeted deletion of the *cer-l* gene. Restriction map of the 129/Sv murine *cer-l* genomic clone, of the targeting construct, and of the recombinant allele. The two targeted exons are depicted here as filled boxes (I and II). The targeting construct contained an IRES-LacZ-Neo cassette and was flanked by 5′ and 3′ homology regions. In addition, an HSV-TK cassette was inserted at the end of the 3′ arm to allow for negative selection. The 5′ and 3′ external probes used in Southern blot analysis, after *Pst* I digest, are shown as white rectangles; the Southern blots confirmed that homologous recombination had taken place. Pairs of PCR primers used to genotype ES cells clones are indicated by arrows. White arrowheads represent PCR primers used for the genotyping of newborns. Bg, *Bgl* II; E, *Eco* RI; H, *Hind* III; K, *Kpn* I; P, *Pst* I. **(b)** Southern blot analysis of DNA obtained from *cer-l* heterozygous intercrosses. DNA was digested with *Pst* I and hybridized with the 3′ external probe. **(c)** PCR analyses of intercrosses. **(d, e)** Dorsal views of the base of the cranium of neonate mouse skeletons stained with Alcian blue and alizarin red: D, low-power view of wild-type neonate; E, same view of a *cer-l*$^{-/-}$ littermate. BO, basioccipital; BS, basisphenoid; PS, presphenoid.

DNA Analysis

DNA was extracted from ES cell clones, mouse newborns or adult tails using standard procedures. Clones presenting proper homologous recombination at the *cer-l* locus were identified by PCR (see Fig. 5) using the following primers: P1-*cer-l*-F (5′-GCT TGG GCT TGT TTC CTT GTG ATG ACT GGT-3′) and P3 IRES-R (5′-TGC TTC CTT CAC GAC ATT CAA CAG ACC TT-3′) for 5′ recombination; P6-Neo-F (5′-GTT CCA CAT ACA CTT CAT TCT CAG-3′) and P4-*cer-l*-R (5′-TAA GGC CTC CAA ACA CAT AGT AAA GTC TCA-3′) for 3′ recombination. Correct targeting was confirmed by Southern blot analysis after *Pst*I digestion using the two external probes indicated in Figure 5.

Genotyping of mouse offspring was routinely determined by PCR using the three oligonucleotides: Mcerl-Eco-Forward (5′-ACC CAC CTG CTG ACC ACC TGC TTC C-3′), Mcerl-L4-Reverse (5′-CTC TTT CTA TTT TGC CGT TTG TC-3′), and P3-IRES-R (indicated as white triangles in Fig. 5), which resulted in bands of 700 and 500 bp for the wild-type and mutant alleles, respectively.

ACKNOWLEDGMENTS

We thank N. Ueno, R. Moon, and D. Melton for gifts of plasmids, K. Masuhara for anti-BMP4 mAb, Genetics Institute for BMPs, K. Lyons for help with the ES cell work, and U.M.T.G. at I.G.C. for help with mouse stocks. S. Marques is supported by a FLAD research fellowship. J.A. Belo, E. Agius, and S. Piccolo were HHMI Associates, of which E.M. De Robertis is an Investigator. This work was supported by grants of the HHMI and the Sprague Endowment to E.M.D.R. and of the Fundação Calouste Gulbenkian/Instituto Gulbenkian de Ciência to J.A. Belo, of which he is a Member Investigator.

LITERATURE CITED

Bachiller D, Klingensmith J, Kemp C., Belo JA, Anderson RM, May SR, McMahon JA, McMahon AP, Harland R, Rossant J, De Robertis EM. 2000. The organizer secreted factors Chordin and Noggin are required for forebrain development in the mouse. Nature 403: 658–661.

Belo JA, Bouwmeester T, Leyns L, Kertesz N, Gallo M, Follettie M, De Robertis EM. 1997. *Cerberus-like* is a secreted factor with neuralizing activity expressed in the anterior primitive endoderm of the mouse gastrula. Mech Dev 68:45–57.

Belo JA, Leyns L, Yamada G, De Robertis EM. 1998. The prechordal midline of the chondrocranium is defective in Goosecoid-1 mouse mutants. Mech Dev 72:15–25.

Biben C, Stanley E, Fabri L, Kotecha, S, Rhinn M, Drinkwater C, Lah M, Wang CC, Nash A, Hilton, D. et al. 1998. Murine Cerberus homologue mCer-1: a candidate anterior patterning molecule. Dev Biol 194:135–151.

Bouwmeester T, Kim SH, Sasai Y, Lu B, De Robertis EM. 1996. Cerberus is a head-inducing secreted factor expressed in the anterior endoderm of Spemann's organizer. Nature 382:595–601.

Bouwmeester T, Leyns L. 1997. Vertebrate head induction by anterior primitive endoderm. BioEssays 19:855–863.

Brannon M, Gomperts M, Sumoy L, Moon RT, Kimelman D. 1997. A beta-catenin/XTcf-3 complex binds to the siamois promoter to regulate dorsal axis specification in Xenopus. Genes Dev 11: 2359–2370.

Chang C, Wilson PA, Mathews, Hemmati-Brivanlou A. 1997. A *Xenopus* Type I activin receptor mediates mesodermal but not neural specification during embryogenesis. Development 124:827–837.

Hsu DR, Economides AN, Wang X, Eimon PM, Harland RM. 1998. The *Xenopus* dorsalizing factor gremlin identifies a novel family of secreted proteins that antagonize BMP activities. Mol Cell 1:673–683.

Kessler DS, Melton DA. 1995. Induction of dorsal mesoderm by soluble, mature Vg1 protein. Development 121:2155–2164.

McKendry R, Hsu SC, Harland RM, Grosschedl R. 1997. LEF-1/TCF proteins mediate wnt-inducible transcription from the Xenopus nodal-related 3 promoter. Dev Biol 192:420–431.

Pearse JJH, Penny G, Rossant J. 1999. A mouse cerberus/Dan-related gene family. Dev Biol 209:98–110.

Piccolo S, Sasai Y, Lu B, De Robertis EM. 1996. Dorsoventral patterning in *Xenopus*: inhibition of ventral signals by direct binding of Chordin to BMP-4. Cell 86:589–598.

Piccolo S, Agius E, Bouwmeester T, Bhattacharyya S, Grunz H, De Robertis EM. 1998. The head inducer Cerberus is a multifunctional antagonist of Nodal, BMP and Wnt signals. Nature 397:707–710.

Robertson EJ. 1987. Embryo-derived stem cell lines. In: Robertson EJ, editor. Teratocarcinomas and embryonic stem cells: a practical approach. Oxford: IRL Press. p 71–112.

Rodriguez-Esteban C, Capdevila J, Economides AN, Pascual J, Ortiz A, Izpisua-Belmonte JC. 1999. The novel Cerberus-like protein Caronte mediates the establishment of embryonic left-right asymmetry. Nature 401:243–251.

Shawlot W, Deng JM, Behringer RR. 1998. Expression of the mouse *cerberus-related* gene, *Cerr1,* suggests a role in anterior neural induction and somitogenesis. Proc Natl Acad Sci 95:6198–6203.

Simpson EH, Johnson DK, Hunsicker P, Suffolk R, Jordan SA, Jackson IJ. 1999. The mouse Cer1 (Cerberus related or homologue) gene is not required for anterior pattern formation. Dev Biol 213:202–206.

Thomas P, Beddington RSP. 1996. Anterior primitive endoderm may be responsible for patterning the anterior neural plate in the mouse embryo. Curr Biol 6:1487–1496.

Tybulewicz VL, Crawford CE, Jackson PK, Bronson R.T, Mulligan RC. 1991. Neonatal lethality and lymphopenia in mice with a homozygous disruption of the c-abl proto-oncogene. Cell 65:1153–1163.

Wilson PA, Hemmati-Brivanlou A. 1995. Induction of epidermis and inhibition of neural fate by BMP-4. Nature 376:331–333.

Yokouchi Y, Vogan KJ, Pearse RV, Tabin CJ. 1999. Antagonistic signaling by Caronte, a novel Cerberus-related gene, establishes left-right asymmetric gene expression. Cell 98:573–583.

Zhu L, Marvin M, Gardiner A, Lassar A, Mercola M, Stern CD, Levin, M. 1999. Cerberus regulates left/right asymmetry of the embryonic head and heart. Curr Biol 9:931–938.

Zimmerman LB, De Jesús-Escobar JM, Harland RM. 1996. The Spemann organizer signal noggin binds and inactivates bone morphogenetic protein-4. Cell 86:599–606.